frontiers | Frontiers in Earth Science

ORIGINAL RESEARCH
published: 02 June 2022
doi: 10.3389/feart.2022.918683

Fracture Identification of Deep Dolomite Reservoir Based on R/S-FD Analysis: A Case Study of the Cambrian Sinian Reservoirs in the Sandaoqiao Gas Field, Northern Tarim Basin

Qingxiu Meng[1,2,3], *Wenlong Ding*[1,2,3]*, *Xindong Diao*[4], *Pengyuan Han*[1,2,3], *Huanhuan Wang*[1,2,3] and *Zikang Xiao*[1,2,3]

[1]School of Energy Resources, China University of Geosciences, Beijing, China, [2]Key Laboratory of Marine Reservoir Evolution and Hydrocarbon Enrichment Mechanism, Ministry of Education, China University of Geosciences, Beijing, China, [3]Beijing Key Laboratory of Unconventional Natural Gas Geological Evaluation and Development Engineering, China University of Geosciences, Beijing, China, [4]Sinopec Northwest Oilfield Company, Urumqi, China

OPEN ACCESS

Edited by:
Wei Ju,
China University of Mining and Technology, China

Reviewed by:
Kun Zhang,
Henan Polytechnic University, China
Jianhua He,
Chengdu University of Technology, China

***Correspondence:**
Wenlong Ding
dingwenlong2006@126.com

Specialty section:
This article was submitted to Structural Geology and Tectonics, a section of the journal Frontiers in Earth Science

Received: 12 April 2022
Accepted: 29 April 2022
Published: 02 June 2022

Citation:
Meng Q, Ding W, Diao X, Han P, Wang H and Xiao Z (2022) Fracture Identification of Deep Dolomite Reservoir Based on R/S-FD Analysis: A Case Study of the Cambrian Sinian Reservoirs in the Sandaoqiao Gas Field, Northern Tarim Basin. Front. Earth Sci. 10:918683. doi: 10.3389/feart.2022.918683

The pre-Mesozoic Sandaoqiao gas field, northern Tarim Basin, Western China, hosts a typical deep fractured dolomite reservoir. Taking this area as an example, this study carried out identification research on the fracture development section of the Cambrian Sinian deep (5,700–6200 m) thick (60–80 m) fractured dolomite reservoirs. The core scale identification and numerical analysis method of heavy gauge finite difference (R/S-FD) are used to identify the fracture development section. In the process of applying this method to the study area, by comparing the fracture development identification results of continuous and complete coring sections, three logging curves with high fracture sensitivity (AC/DEN/CAL) are selected. The adjusted R/S-FD analysis method can effectively identify the fracture development section of the fractured dolomite reservoir. Among them, five fracture development sections were identified in well Q1, with an average thickness of 6.8 m. The fracture development section is in good consistency with the reservoir interpretation section of conventional logging. Well, Q101 identified 11 fracture development sections with an average thickness of 2.5 m. The results show that the gas logging section lags behind the fracture development section, mainly corresponding to the lower part of the identified fracture development section. The thickness and distribution of the longitudinal fracture development section of the two wells are obviously different. The research shows that the R/S-FD method can well identify the fracture development section of a fractured dolomite reservoir.

Keywords: rescaled range analysis, R/S-FD method, fracture identification, fractured dolomite reservoir, sandaoqiao gas field

INTRODUCTION

Carbonate reservoirs are one of the most important reservoir types in the world (Zhu et al., 2020). Dolomite reservoir is one of the common carbonate reservoir types (Antonellini and Mollema, 2000; Ma et al., 2008; Guo et al., 2020). Compared with limestone, this kind of reservoir facies is more brittle and has weak dissolution (Zheng H. et al., 2007; Zheng R. C. et al., 2007; Davies and Smith, 2011). The main reservoir space of the Cambrian Sinian reservoir in the sandaoqiao gas field is mainly fractured, and a typical fractured dolomite reservoir is developed. Structural fractures directly affect the quality and production of dolomite reservoirs.

Fractures in reservoirs are the key to high and stable production of oil and gas reservoirs, especially for tight sandstone, shale, and carbonate reservoirs (Chen et al., 2021; Lai et al., 2020; Song et al., 2015; Zhou et al., 2020; Liu et al., 2022; Zhou et al., 2022). The development degree and distribution characteristics of fractures directly affect the physical properties and production of oil and gas reservoirs. In recent years, fractures have always been the focus of reservoir research (Luo et al., 2012; Yin and Wu., 2020; Zhao et al., 2021; Wang et al., 2022). Identifying the characteristics of fracture development sections in underground reservoirs vertically is one of the research contents (Prioul and Jocker, 2009; Santos et al., 2015; Fernández-Ibanez et al., 2018; He et al., 2020; Wang et al., 2021; Yin et al., 2020).

There are many ways to identify the fracture development section longitudinally (Hong et al., 2020; Lan et al., 2021; Zheng et al., 2020; Li, 2022). These methods include geological outcrop, core, logging data, and seismic data (Aghli et al., 2016; Bates et al., 1999; Lai et al., 2017; Liu et al., 2019; Yin et al., 2018a; Li H. et al., 2020; Li, 2022). Considering the recognition accuracy, recognition range, representativeness, cost, and other factors, the use of conventional logging curves is more practical and economical (Miranda and Andrade, 1999; Zhao et al., 2011; Ding et al., 2012; Ding et al., 2013; Xue et al., 2014; Yang et al., 2017; Yin et al., 2018b; Afshari et al., 2018). R/S method uses several conventional logging curves sensitive to fracture response to identify fracture development sections (Mandelbrot and Wallis, 1969; Li et al., 2018; Xiao et al., 2019a; Xiao et al., 2019b; Li et al., 2019; Zhao et al., 2019). The finite difference method improves the accuracy and effect of the R/S method. R/S-FD method is used to identify the longitudinal fracture development section of a single well, and its application in shale and tight sandstone reservoirs is relatively mature (Wang et al., 2018; Xiao et al., 2019a; Li et al., 2019). This study applies this method to a deep fractured dolomite reservoir for the first time. The results have also been verified by other reservoir interpretation methods.

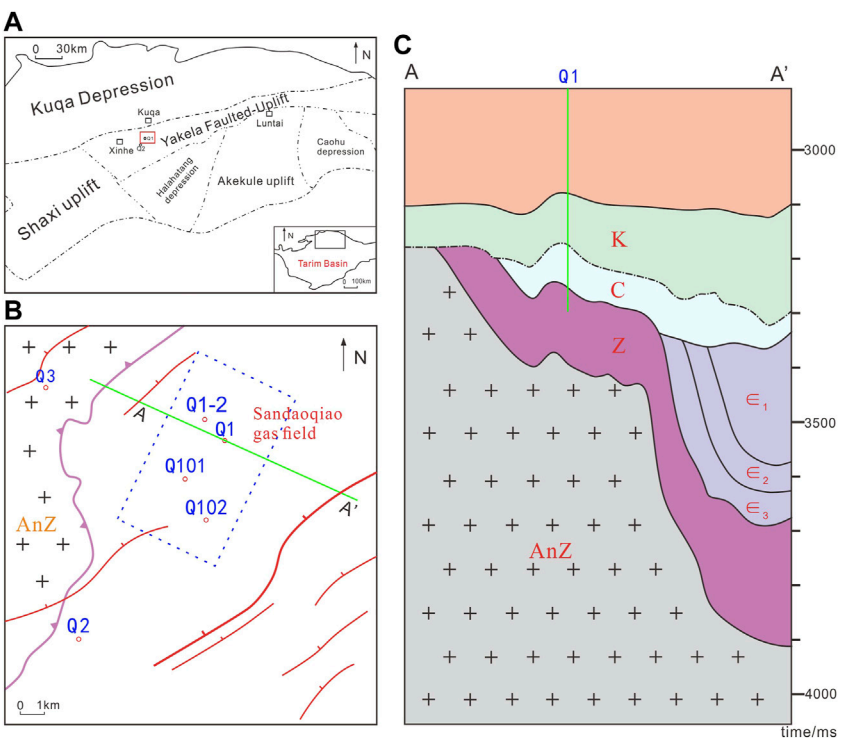

FIGURE 1 | (A) Structural location of sandaoqiao gas field. **(B)** Stratigraphic elements and well location distribution map of the Cretaceous bottom boundary. The red line is the main fault, and the purple line is the Sinian pinch-out line. **(C)** NW-SE direction section AA' stratigraphic structure diagram. The green line is the trajectory of key well Q1.

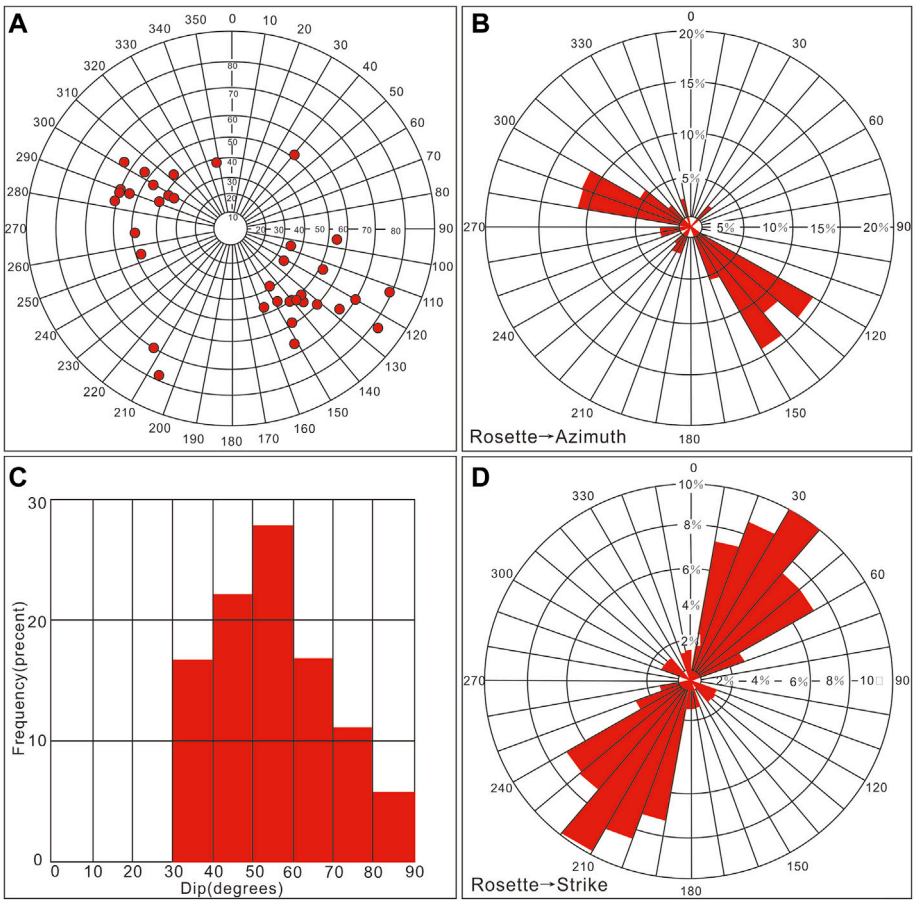

FIGURE 2 | Fracture parameter statistics of Q1 well based on imaging logging. **(A)** The azimuth distribution of fractures was identified by imaging logging in the Q1 well. **(B)** The distribution of fracture tendency is shown in the rose diagram. **(C)** Statistical distribution of fracture dip angle. **(D)** The distribution of fracture strikes is shown in the rose diagram. Imaging logging shows that there are 36 fractures in well Q1, with an average dip angle of 76° and an average dip of 314°.

GEOLOGICAL SETTING

The Tarim Basin is located in western China and is an important developing oil- and gas-producing area. The Sandaoqiao gas field is located in the northern Tarim Basin (**Figure 1**), in the western part of the Yakela Faulted Uplift (Han et al., 2016; Yang et al., 2018). The Kuqa depression is located to the north, and the Halahatang depression is located to the south. The Sandaoqiao gas field is generally located in the compression-derived structural slope of the far margin uplift of the foreland basin. The Sinian system of the Cambrian system was severely eroded with the formation of a structural compression fold, forming a buried hill drape structure (Li Y. et al., 2020; Wang et al., 2021), with a reservoir characterized by a denuded residual buried hill (**Figure 1**). The Cambrian Sinian strata are pinched out on the Yakela Faulted-Uplift oriented in the NW direction (Han et al., 2015). The Carboniferous strata overlying the Sandaoqiao gas field are compact and stable, with good caprock conditions, which prevented the surface water from leaching and dissolving Cambrian Sinian strata during the regional long-term denudation period. These conditions have formed a condensate gas reservoir producing area with a Carboniferous cap rock and developed structural fractures.

In the study area, the depth of the Cambrian Sinian system is 5,700–6,200 m, which is deep-ultradeep. The thickness of the Cambrian Sinian strata is uniform. From the late Paleozoic to Mesozoic, this stratum experienced multiple superimposed weak-strong thrusting fault events, accompanied by strong weathering and denudation. The Mesozoic Cretaceous strata cover formed a denudation residual buried hill drape structure. The lithology is characterized by the development of deeply fractured dolomite reservoirs (micritic and powdery). According to the measured physical property data, the porosity and permeability of dolomite reservoirs in the study area are relatively low. Structural fracture is the main reservoir space. The properties of the structural fractures are considered the key factors in determining the reservoir space and seepage performance.

Characteristics of Tectonic Stress

In the geological history period, the study area was mainly affected by NW strong compressive stress and pre-Mesozoic

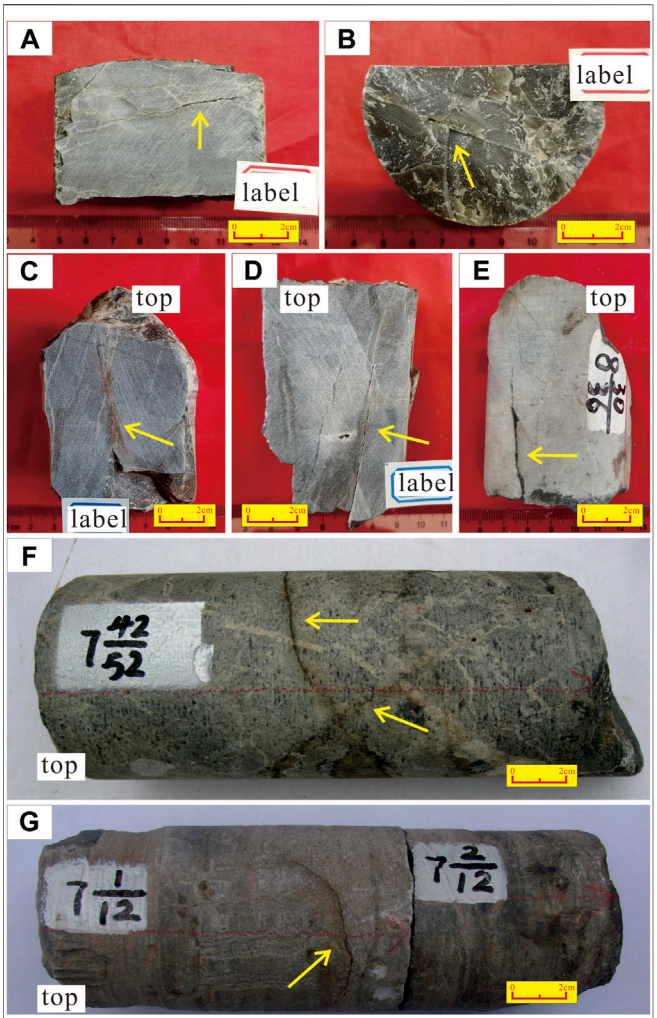

FIGURE 3 | Fracture development characteristics from core sections in the Sandaoqiao gas field. **(A,B)**, well Q1, Z, 5,754.8 m, gray fine-grained dolomite, half-filled fracture; **(C)**, well Q101, ϵ, 5,758 m, light-red-oil-trace dolomite, high-angle fracture; **(D)**, well Q101, ϵ, 5,761.04 m, gray-black-oil-trace silty siliceous dolomite, high-angle fracture development, half-filled; **(E)**, well Q101, ϵ, 5,761.08 m, gray-black-oil-trace silty siliceous dolomite. **(F)**, well, Q1, Z, 5,753.98–5,754.14 m, two intersecting oblique fractures with a width of 0.1–0.5 mm; **(G)**; well, Q101, ϵ, 5,757–5,757.19 m, gray-black calcareous dolomite, 1 inclined fracture, approximately 8 cm in length and 0.1 mm in width.

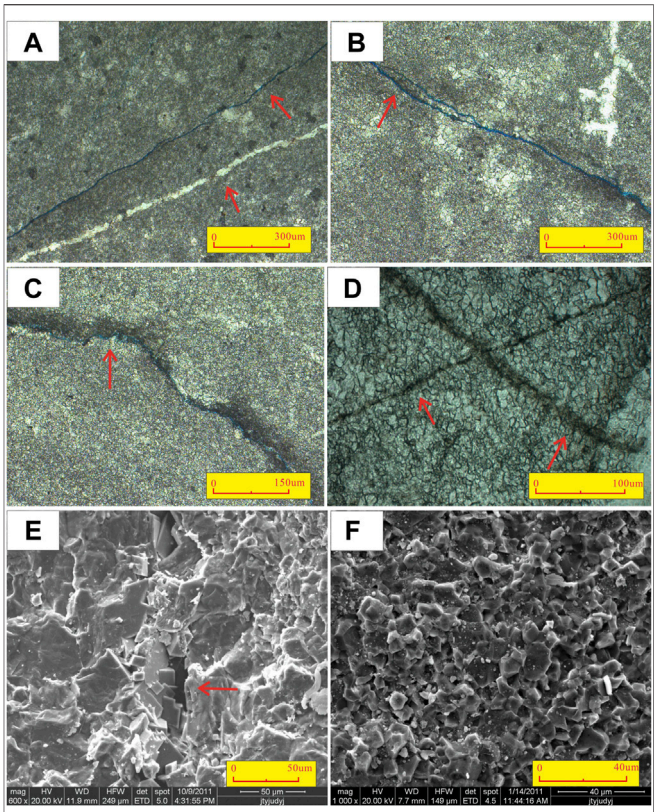

FIGURE 4 | Fracture development characteristics from cast thin sections and SEM in the Sandaoqiao gas field. **(A)**, well Q1, Z, 5,741.4 m, argillaceous dolomite; 3% continental debris, 1% siliceous, and 1% muscovite. Three microcracks were filled with siliceous material and 1 microcrack was filled with dolomite. **(B)**, well Q1, Z, 5,754.8 m, silty argillaceous dolomite, 2% siliceous, and 1% muscovite. The face rate is less than 1%. One microcrack with a width of 0.01 mm. **(C)**, well Q1, Z, 5,756.1 m, silty argillaceous dolomite, 2% siliceous, and 1% muscovite. The face rate is less than 1%. One straight microcrack with a width less than 0.01 mm; one microcrack along the suture, with a width less than 0.01 mm; **(D)**, well Q101, ϵ, 5,821.5 m, the dolomite grains are 0.04–0.10 mm, granular and inlaid. Microcracks are developed. Dolomite; **(E)**, well Q101, ϵ, 5,822.2 m, dolomite-filled fractures, part of which have clay on the surfaces, dolomite with poor crystallization, generally semi-automorphic-heteromorphic; **(F)**, well Q1, Z,5,741.4 m, gray micrite dolomite, argillaceous dolomite, dolomite with poor crystallization, generally semi-automorphic-heteromorphic.

strong denudation, forming a buried hill drape structure with strata pinching out in the NW direction.

According to the analysis results of imaging logging and other logging data, the azimuth of the fast shear wave is NE, and the induced fractures thus strike NE. It is comprehensively inferred that the horizontal principal stress direction is NE. The NE trending fault strike (**Figure 2**) is roughly consistent with the current horizontal principal stress direction.

Fracture Characteristics

According to the seismic data, the main faults in the study area are NE-trending, and most of them terminate in the upper Cambrian strata. They are mainly high-angle and oblique parallel reverse faults with lower-order faults.

The fracture development of the core sections of wells Q1 and Q101 in fine crystalline powder dolomite has resulted in mainly high-angle and half-filled fractures (**Figure 3**), and conjugate fractures are found locally. The total length of the observed core is 50.3m, and the average coring rate is 76%. We analyzed and photographed all coring sections. Dissolution pores are rare.

The cast thin sections show that the dolomite dissolution in this section is very weak (**Figure 4**). We observed and analyzed a total of 16 cast thin sections, 7 ordinary thin sections, and 10 SEM analysis reports. The typical fracture development parts in the study area are selected for sampling. It is clear that the fractured dolomite reservoir is the main feature in this section of the

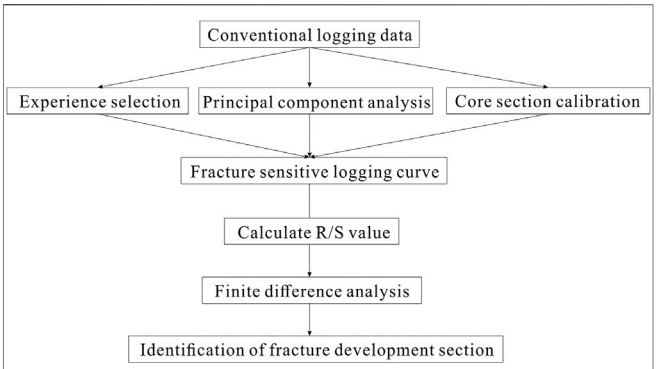

FIGURE 5 | Process of identifying fracture development section based on R/S-FD method.

Sandaoqiao gas field. The scanning electron microscopy (SEM) results showed that there were microcracks in some parts of the section. This dolomite is generally subhedral heteromorphic, without obvious dissolution.

METHODOLOGY

R/S-FD Method

The numerical analysis method used in this study is based on the R/S method. In R/S analysis, R is the range, that is, the difference between the maximum cumulative deviation and the minimum cumulative deviation, representing the complexity of the time series; S is the standard deviation, that is, the square root of the change, representing the average trend of the time series (Hurst. 1951; Pang and North, 1996). The ratio of the range to the standard deviation (i.e., the rescaling range R/S) represents a dimensionless time series and the fluctuation intensity (Xiao et al., 2019a; Yang et al., 2020).

$$R(\mathrm{n}) = \max_{0<\mathrm{u}<\mathrm{n}}\left\{\sum_{i=1}^{u} Z(i) - \frac{\mathrm{u}}{\mathrm{n}}\sum_{i=1}^{u} Z(j)\right\} - \min_{0<\mathrm{u}<\mathrm{n}}\left\{\sum_{i=1}^{u} Z(i) - \frac{\mathrm{u}}{n}\sum_{i=1}^{u} Z(j)\right\} \quad (1)$$

$$\mathrm{S}(\mathrm{n}) = \sqrt{\frac{1}{\mathrm{n}}\sum_{i=1}^{u} Z^2(i) - \left[\frac{1}{n}\sum_{j=1}^{u} Z(j)\right]^2} \quad (2)$$

The concave section of the R(n)/S(n) curve can be regarded as the location of fracture development. To avoid recognition error, the R/S-FD method uses the finite difference method to calculate the second derivative of these discrete data (Xiao et al., 2019a). The zone with a positive second derivative can be identified as a fracture development section. F is the multiplication of the K value of the multigroup logging curve, which represents the accumulation of the fracture development probability of multigroup logging data identification.

The basic data of the R/S-FD method is a conventional logging curve. Firstly, the crack sensitivity curve suitable for the study area is selected by various methods. On the basis of referring to several commonly used fracture sensitivity curves, this study first uses the fracture development of the coring section to restrict the curve selection and selects three fracture sensitivity curves (DEN, AC, and CAL) to calculate the K value. Considering that the sampling interval of logging data is mostly 0.1 or 0.125 m, it is of certain indicative significance to optimize the fracture sensitivity curve by using whether there are fractures in the core section with a certain length (0.3–0.5 m). Then calculate the R/S value of the logging data of the study interval, and carry out the finite difference calculation (**Figure 5**). Finally, the calculated F value is used to identify the fracture development section.

Data Selection and Calculation

The following factors are considered in the selection of the numerical analysis method. The pre-Mesozoic Cambrian Sinian system in the study area is the main body of a large set of dolomites with single and continuous lithologic structures. Unlike tight sandstone/shale sections, the dolomite reservoir in the study area does not include lithology mutation surfaces such as sand-mud interbedding surfaces. The reservoir as a whole is a fractured dolomite reservoir with undeveloped pores (based on the 50.3 m coring data of four wells in the Sandaoqiao gas field and imaging logging data, the pores are undeveloped). The interference of holes is eliminated. The logging curve is complete, and the quality of the logging core data is good. The combination of R/S logging and core analysis is suitable.

Taking well Q1 as an example, the double logarithm curve of R/S value and serial number is made, and seven kinds of logging curves are selected for this analysis (**Figure 6**). The sensitivity of different good logs to fracture development varies. At the same

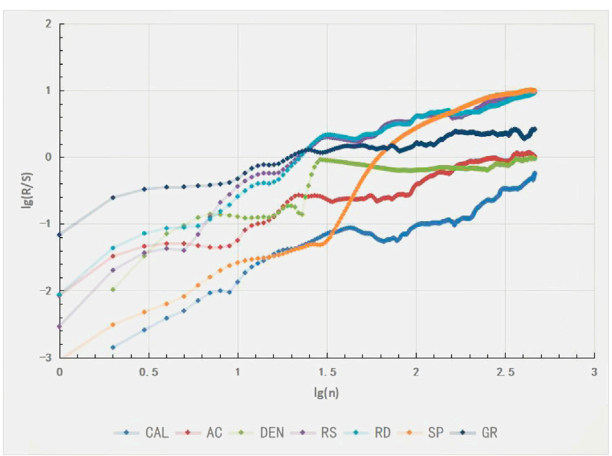

FIGURE 6 | Double logarithm curve of the R/S calculation results of multiple logging curves in well Q1. In this method, the concave section of the curve is identified as the fracture development section. AC is the acoustic log, DEN is the density log, CAL is the caliper log, SP is the spontaneous potential log, GR is the natural gamma log, RS is the shallow lateral resistivity log and RD is the deep lateral resistivity log.

TABLE 1 | Recognition effect of various logging curves on the fracture development depth of the coring section.

Well Name	Coring depth section/m	Core length/m	Fracture development	Recognition (corresponding o/Non-corresponding ×)						
				AC	DEN	CAL	RS	RD	SP	GR
Q1	5,741.1–5,741.4	0.3	Yes	O	o	o	o	o	×	o
Q1	5,745.6–5,746	0.4	Yes	O	o	o	o	o	o	o
Q1	5,747.3–5,747.7	0.4	Yes	O	o	o	o	o	×	o
Q1	5,749–5,749.3	0.3	Yes	O	o	o	×	×	×	×
Q1	5,753.7–5,754	0.3	Yes	O	o	o	×	×	×	o
Q1	5,754.5–5,754.8	0.3	Yes	O	o	o	×	×	×	o
Q1	5,756.1–5,756.4	0.3	Yes	O	o	o	o	o	o	o
Q1	5,757.8–5,758.2	0.4	Yes	O	o	o	×	×	o	o
Q1	5,759.7–5,760	0.3	Yes	O	o	o	o	o	o	o
Q1	5,763.8–5,764.1	0.3	Yes	O	o	o	×	×	×	×
Q101	5,757.8–5,758.1	0.3	Yes	O	o	o	o	o	o	×
Q101	5,760.6–5,761.1	0.5	Yes	O	o	o	o	o	o	o

Table 1 *shows that the commonly used fracture sensitivity curves AC, DEN, and CAL are consistent in the identification of fracture development section in the core section. The other four kinds of curves show a relatively low recognition rate for the fracture development section.*

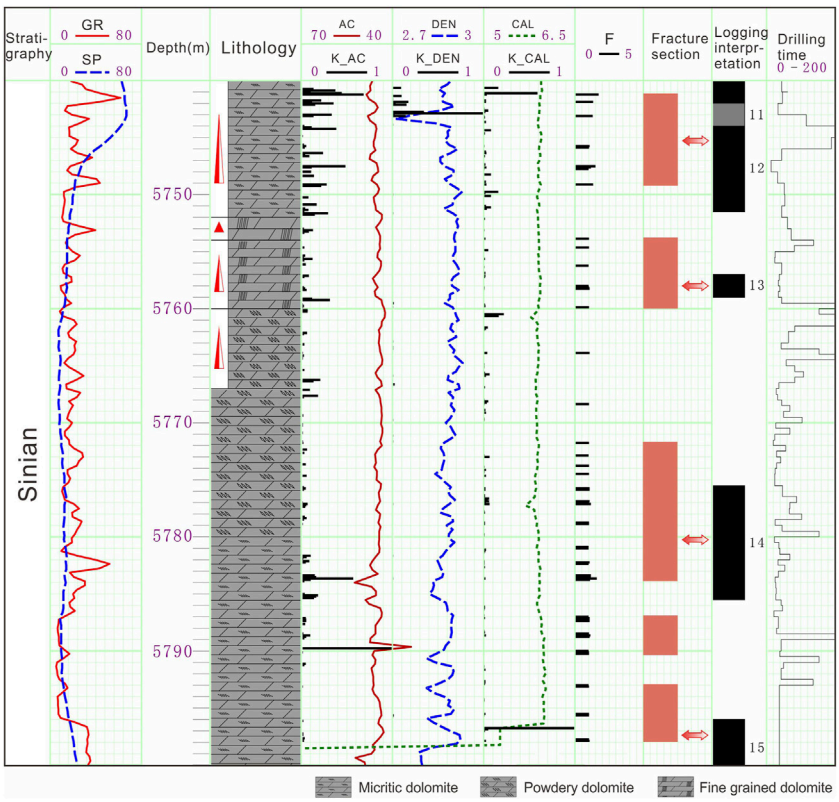

FIGURE 7 | Results of fracture development section identified with the R/S-FD method in well Q1. The red and white double arrows show the corresponding relationship between the fracture development section and the conventional logging interpretation section.

time, the difference in lithofacies between study areas will make the analysis effect of different logging curves different.

Seven kinds of logging curves are selected in the analysis of wells Q1 and Q101: the CAL, AC, and DEN curves, which are widely used in R/S analysis, and other control curves RS, RD, SP, and GR. After comparing and analyzing the calculation results of the confirmatory fracture development section and logging curve in the coring section, CAL, AC and DEN are selected as the research objects (**Table 1**). That is, the F value used in this study is a product of the CAL, AC, and DEN K values (K_CAL/K_AC/K_DEN). In the fracture development section, the identification result with good applicability is obtained.

$$F = K_{AC} * K_{DEN} * K_{CAL} \tag{3}$$

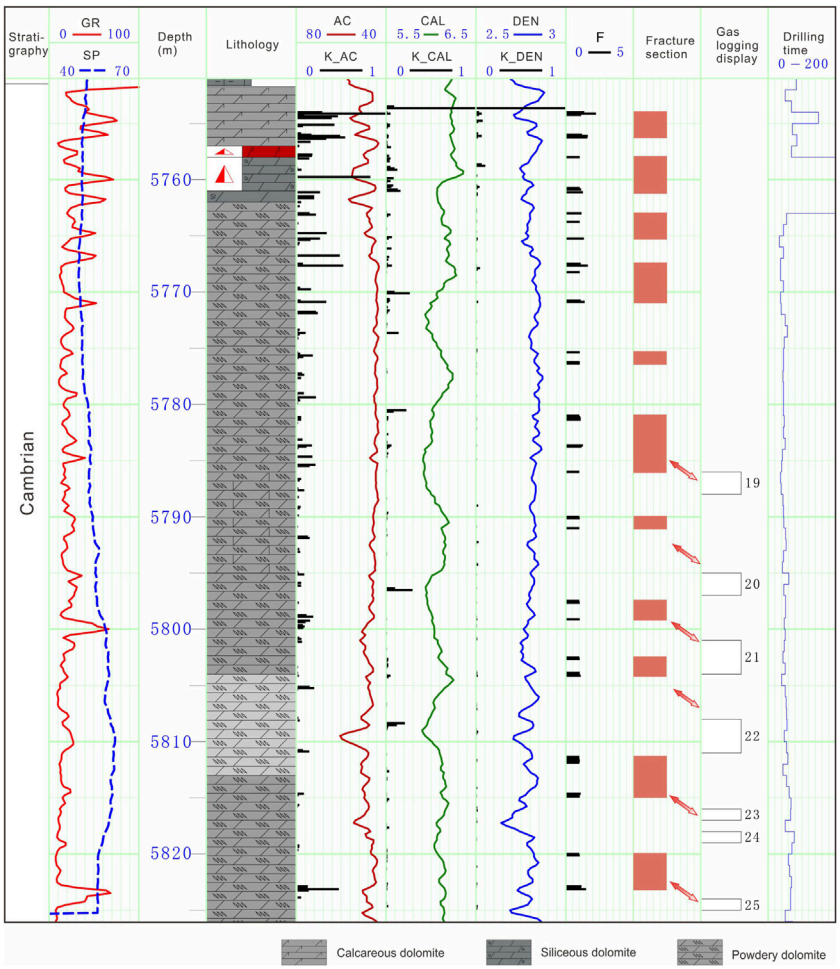

FIGURE 8 | Fracture development results identified with the R/S-FD method in well Q101. The red and white double arrows show the corresponding relationship between the fracture development section and the gas logging display section.

The calculation method used in this study is adjusted on the basis of the R/S-FD method. Based on the particularity of the dolomite value, the value range is adjusted, and the K value calculated by the logging curve at this depth is smaller (this may be related to the particularity of dolomite logging curves, with a small number of especially large or small values). Because K represents the fluctuation in logging data, we homogenize the interval of $k > 0$ to 1-2, which makes the probability of fracture development accumulate positively. If $k = 0$, then $F = 0$; if $K \neq 0$, then F is the product of the K values of the CAL, AC, and DEN. Thus, the fracture development section can be clearly identified.

RESULTS

Characteristics of the Fracture Development Section

The dolomite section of well Q1 has developed thick fractures (a 60 m section), which can be divided into five sections, with an average thickness of 6.8 m and an average fracture spacing of 5.6 m (**Figure 7**). The fracture development section of well Q1 is relatively thicker and denser. The fractures of the core of well Q1 are high-angle and half-filled. The vertical distribution of the fracture development section in well Q101 is relatively uniform (an 80 m section), which can be divided into 11 sections, and the thickness of these fractures is thinner than those in well Q1, with an average length of 2.5 m and an average spacing of 4.1 m (**Figure 8**). Relatively speaking, the fracture development section of well Q101 is thinner and more dispersed.

Correlation Between the Fracture Development Section and Actual Production Data

The R/S-FD method is used to analyze the fractured dolomite reservoir of the Cambrian Sinian system in the Sandaoqiao area. The results show that the comprehensive identification results of multiple logging curves are in good correspondence with the actual observation results of cored sections, traditional numerical logging interpretations, and gas logging displays.

The fracture development section identified by well Q1 shows a good correspondence with the reservoir section interpreted by traditional logging data. The identified fracture development section corresponds to logging interpretation reservoir section Nos. 11–15 (**Figure 7**). The lower gas logging section of the dolomite reservoir in the Q101 well has a good correspondence with the identified fracture development section, corresponding to gas logging section Nos. 19–25 and in the lower part of the identified fracture development section, lagging behind the fracture development section (**Figure 8**). This correspondence shows that the R/S-FD method has certain applicability in fractured dolomite reservoirs.

DISCUSSION

Fracture Types

The fracture types in the fracture development section identified by the R/S-FD method are noteworthy information (Xiao et al., 2019a). Through the identification results of Q1 and Q101 wells, combined with core, imaging logging, and other data, it is considered that most of the identified fractures are medium high angle fractures, semi filled and unfilled. Part of the fractures generated under the compression of the early formation are completely filled in the later stage. Because the filling material is similar to the composition of the reservoir, it is less abnormal in density logging and caliper logging. The identification effect of this method on this kind of fracture is general.

Controlling Factors

The difference between the two wells in the characteristics of longitudinal fracture development sections is affected by many factors, mainly including lithology, structural position, structural stage, and so on (Zhao et al., 2019). In addition, compared with the two wells, well Q1 shows higher and more stable oil and gas production. This difference may be due to the greater thickness of the average fracture development section of well Q1.

Method Applicability

The R/S-FD method also shows its limitations in the application of different strata in different areas (Xiao et al., 2019a; Li et al., 2019; Yang et al., 2020). Firstly, the stratum thickness used to identify the fracture development section should not be too thick. With the increase of thickness, reservoir heterogeneity is also increasing, which will make the anomalies identified by the R/S method contain a variety of other information. Secondly, the lithology of the study interval should be unified as far as possible. The sudden change in lithology will bring complex changes to the logging curve, which will reduce the accuracy of R/S recognition. In the application of the dolomite stratum, it is generally considered that a thickness less than 100 m is more suitable. In the fracture identification of the 300 m reservoir section of well Q102, the results show that the spacing of fracture development sections is too large, and there is no good corresponding result in the comparison with the coring section and production means.

CONCLUSION

1. In this study, the adjusted R/S-FD method is applied to fractured dolomite reservoirs in the deep layer (5,700–6200 m) of the Cambrian Sinian system (60–80 m), and good recognition results are obtained. In the process of applying this method to the study area, by comparing the fracture development identification results of continuous and complete coring sections, three logging curves with high fracture sensitivity (AC/DEN/CAL) are selected.

2. The adjusted R/S-FD analysis method can effectively identify the fracture development section of the fractured dolomite reservoir. Among them, five fracture development sections were identified in well Q1, with an average thickness of 6.8 m. The fracture development section is in good consistency with the reservoir interpretation section of conventional logging. Well, Q101 identified 11 fracture development sections with an average thickness of 2.5 m. The results show that the gas logging section lags behind the fracture development section, mainly corresponding to the lower part of the identified fracture development section. The difference between the two wells in the characteristics of longitudinal fracture development sections is affected by many factors, mainly including lithology, structural position, structural stage, and so on.

DATA AVAILABILITY STATEMENT

The original contributions presented in the study are included in the article/Supplementary Material; further inquiries can be directed to the corresponding author.

AUTHOR CONTRIBUTIONS

WD and QM are responsible for the idea and writing of this study and XD, PH, HW, and ZX are responsible for the logging interpretation.

FUNDING

This research was supported by the National Natural Science Foundation of China (Grant No. 42072173) and the National Sciences and Technology Major Project of China (2016ZX05046-003-001).

ACKNOWLEDGMENTS

The authors thank the staff of all of the laboratories that cooperated in performing the tests and analyses. We are also grateful to the reviewers, whose comments improved the quality of this manuscript.

REFERENCES

Afshari, M. J., Somogyvári, M., Valley, B., Jalali, M., Loew, S., and Bayer, P. (2018). Fracture Network Characterization Using Stress-Based Tomography. *J. Geophys. Res. Solid Earth* 123, 9324–9340. doi:10.1029/2018JB016438

Aghli, G., Soleimani, B., Moussavi-Harami, R., and Mohammadian, R. (2016). Fractured Zones Detection Using Conventional Petrophysical Logs by Differentiation Method and its Correlation with Image Logs. *J. Petroleum Sci. Eng.* 142, 152–162. doi:10.1016/j.petrol.2016.02.002

Antonellini, M., and Mollema, P. N. (2000). A Natural Analog for a Fractured and Faulted Reservoir in Dolomite: Triassic Sella Group, Northern italy. *Aapg Bull.* 84 (3), 314–344. doi:10.1306/c9ebcddd-1735-11d7-8645000102c1865d

Bates, C. R., Lynn, H. B., and Simon, M. (1999). The Study of a Naturally Fractured Gas Reservoir Using Seismic Techniques. *AAPG Bull.* 83 (9), 1392–1406. doi:10.1306/e4fd41c5-1732-11d7-8645000102c1865d

Chen, G. B., Li, T., Yang, L., Zhang, G. H., Li, J. W., and Dong, H. J. (2021). Mechanical Properties and Failure Mechanism of Combined Bodies with Different Coal-Rock Ratios and Combinations. *J. Min. Strata Control Eng.* 3 (2), 023522. doi:10.13532/j.jmsce.cn10-1638/td.20210108.001

Davies, G. R., and Smith, L. B. (2006). Structurally Controlled Hydrothermal Dolomite Reservoir Facies: an Overview. *Bulletin* 90 (11), 1641–1690. doi:10.1306/05220605164

Ding, W., Li, C., Li, C., Xu, C., Jiu, K., Zeng, W., et al. (2012). Fracture Development in Shale and its Relationship to Gas Accumulation. *Geosci. Front.* 3 (001), 97–105. doi:10.1016/j.gsf.2011.10.001

Ding, W., Zhu, D., Cai, J., Gong, M., and Chen, F. (2013). Analysis of the Developmental Characteristics and Major Regulating Factors of Fractures in Marine-Continental Transitional Shale-Gas Reservoirs: A Case Study of the Carboniferous-Permian Strata in the Southeastern Ordos Basin, Central China. *Mar. Petroleum Geol.* 45, 121–133. doi:10.1016/j.marpetgeo.2013.04.022

Fernández-Ibáñez, F., DeGraff, J. M., and Ibrayev, F. (2018). Integrating Borehole Image Logs with Core: A Method to Enhance Subsurface Fracture Characterization. *Bulletin* 102 (06), 1067–1090. doi:10.1306/0726171609317002

Guo, R., Zhang, S., Bai, X., Wang, K., Sun, X., and Liu, X. (2020). Hydrothermal Dolomite Reservoirs in a Fault System and the Factors Controlling Reservoir Formation-A Case Study of Lower Paleozoic Carbonate Reservoirs in the Gucheng Area, Tarim Basin. *Mar. Petroleum Geol.* 120, 104506. doi:10.1016/j.marpetgeo.2020.104506

Han, Q., Li, Z., Wang, C., Yang, Z.-C., Yan, L., Meng, Q.-L., et al. (2016). Characteristics and Age of a Proterozoic Buried Hill Reservoir in the Northern Shaya Uplift of the Tarim Basin. *Geol. China* 43 (2), 486–499. (in Chinese with English abstract). doi:10.12029/gc20160210

Han, Q., Li, Z., Yang, Z., Yan, L., Shi, Y., and Su, J. (2015). Characteristics of Hydrocarbon Accumulation in the Sandaoqiao Area of Tarim Basin. *Petroleum Geol. Recovery Effic.* 22 (006), 14–20. (in Chinese with English abstract). doi:10.3969/j.issn.1009-9603.2015.06.003

He, X., Zhang, P., He, G., Gao, Y., Liu, M., Zhang, Y., et al. (2020). Evaluation of Sweet Spots and Horizontal-Well-Design Technology for Shale Gas in the Basin-Margin Transition Zone of Southeastern Chongqing, SW China. *Energy Geosci.* 1 (3–4), 134–146. doi:10.1016/j.engeos.2020.06.004

Hong, D., Cao, J., Wu, T., Dang, S., Hu, W., and Yao, S. (2020). Authigenic Clay Minerals and Calcite Dissolution Influence Reservoir Quality in Tight Sandstones: Insights from the Central Junggar Basin, NW China. *Energy Geosci.* 1 (1–2), 8–19. doi:10.1016/j.engeos.2020.03.001

Hurst, H. E. (1951). Long Term Storage Capacity of Reservoirs. *Am. Soc. Civ. Eng. Tans* 116, 776–808. doi:10.1061/taceat.0006518

Lai, J., Chen, K., Xin, Y., Wu, X., Chen, X., Yang, K., et al. (2021). Fracture Characterization and Detection in the Deep Cambrian Dolostones in the Tarim Basin, china: Insights from Borehole Image and Sonic Logs. *J. Petroleum Sci. Eng.* 196, 107659. doi:10.1016/j.petrol.2020.107659

Lai, J., Fan, Z., Wang, Z., Chen, J., Zhou, Z., et al. (2017). Fracture Detection in Oil-Based Drilling Mud Using a Combination of Borehole Image and Sonic Logs. *Mar. Petroleum Geol.* 84, 195–214. doi:10.1016/j.marpetgeo.2017.03.035

Lan, S. R., Song, D. Z., Li, Z. L., and Liu, Y. (2021). Experimental Study on Acoustic Emission Characteristics of Fault Slip Process Based on Damage Factor. *J. Min. Strata Control Eng.* 3 (3), 033024. doi:10.13532/j.jmsce.cn10-1638/td.20210510.002

Li, A., Ding, W., Luo, K., Xiao, Z., Wang, R., Yin, S., et al. (2019). Application of R/S Analysis in Fracture Identification of Shale Reservoir of the Lower Cambrian Niutitang Formation in Northern Guizhou Province, South China. *Geol. J.* 55, 4008–4020. doi:10.1002/gj.3648

Li, H., Qin, Q., Zhang, B., Ge, X., Hu, X., Fan, C., et al. (2020). Tectonic Fracture Formation and Distribution in Ultradeep Marine Carbonate Gas Reservoirs: A Case Study of the Maokou Formation in the Jiulongshan Gas Field, Sichuan Basin, Southwest China. *Energy fuels.* 34 (11), 14132–14146. doi:10.1021/acs.energyfuels.0c03327

Li, H. (2022). Research Progress on Evaluation Methods and Factors Influencing Shale Brittleness: A Review. *Energy Rep.* 8, 4344–4358. doi:10.1016/j.egyr.2022.03.120

Li, J. Z., Laubach, S. E., Gale, J. F. W., and Marrett, R. A. (2018). Quantifying Opening-Mode Fracture Spatial Organization in Horizontal Wellbore Image Logs, Core and Outcrop: Application to Upper Cretaceous Frontier Formation Tight Gas Sandstones, usa. *J. Struct. Geol.* 108, 137–156. doi:10.1016/j.jsg.2017.07.005

Li, Y., Zhou, D., Wang, W., Jiang, T., and Xue, Z. (2020). Development of Unconventional Gas and Technologies Adopted in China. *Energy Geosci.* 1 (1–2), 55–68. doi:10.1016/j.engeos.2020.04.004

Liu, J., Ding, W., Xiao, Z., and Dai, J. (2019). Advances in Comprehensive Characterization and Prediction of Reservoir Fractures. *Prog. Geophys.* 34, 2283–2300. (in Chinese with English abstract). doi:10.6038/pg2019CC0290

Liu, Z., Zhang, Y., and Zhang, Y. (2022). Influencing Factor Analysis on the Fractured Tight Sandstone Gas Reservoir Characteristics: A Case Study of Bozi 3 Gas Reservoir in the Tarim Basin. *Front. Earth Sci* 10, 881934. doi:10.3389/feart.2022.881934

Luo, X., Tang, L., and Xie, D. (2012). Mesozoic Bottom Boundary Unconformity and its Significance for Hydrocarbon Exploration in the Yakela Faulted uplift,Tarim Basin. *Oil Gas Geol.* 33 (1), 30–36. (in Chinese with English abstract). doi:10.11743/ogg20120104

Ma, Y., Guo, T., Zhao, X., and Cai, X. (2008). The Formation Mechanism of High-Quality Dolomite Reservoir in the Deep of Puguang Gas Field. *Sci. China Ser. D-Earth Sci.* 51 (1), 53–64. doi:10.1007/s11430-008-5008-y

Mandelbrot, B. B., and Wallis, J. R. (1969). Robustness of the Rescaled Range R/s in the Measurement of Noncyclic Long Run Statistical Dependence. *Water Resour. Res.* 5 (5), 967–988. doi:10.1029/WR005i005p00967

Miranda, J. G. V., and Andrade, R. F. S. (1999). Rescaled Range Analysis of Pluviometric Records in Northeast brazil. *Theor. Appl. Climatol.* 63 (1-2), 79–88. doi:10.1007/s007040050094

Pang, J., and North, C. P. (1996). Fractals and Their Applicability in Geological Wireline Log Analysis. *J. Pet. Geol.* 19 (3), 339–350. doi:10.1111/j.1747-5457.1996.tb00438.x

Prioul, R., and Jocker, J. (2009). Fracture Characterization at Multiple Scales Using Borehole Images, Sonic Logs, and Walkaround Vertical Seismic Profile. *Bulletin* 93, 1503–1516. doi:10.1306/08250909019

Santos, R. F. V. C., Miranda, T. S., Barbosa, J. A., Gomes, I. F., Matos, G. C., Gale, J. F. W., et al. (2015). Characterization of Natural Fracture Systems: Analysis of Uncertainty Effects in Linear Scanline Results. *Bulletin* 99 (12), 2203–2219. doi:10.1306/05211514104

Song, D., Wang, T.-G., and Li, H. (2015). Geochemical Characteristics and Origin of the Crude Oils and Condensates from Yakela Faulted-Uplift, Tarim Basin. *J. Petroleum Sci. Eng.* 133, 602–611. doi:10.1016/j.petrol.2015.07.007

Wang, S., Wang, G., Lai, J., Li, D., Liu, S., Chen, X., et al. (2020). Logging Identification and Evaluation of Vertical Zonation of Buried Hill in Cambrian Dolomite Reservoir: A Study of Yingmai-Yaha Buried Hill Structural Belt, Northern Tarim Basin. *J. Petroleum Sci. Eng.* 195, 107758. doi:10.1016/j.petrol.2020.107758

Wang, X., Ding, W., Cui, L., Wang, R., He, J., Li, A., et al. (2018). The Developmental Characteristics of Natural Fractures and Their Significance for Reservoirs in the Cambrian Niutitang Marine Shale of the Sangzhi Block, Southern china. *J. Petroleum Sci. Eng.* 165, 831–841. doi:10.1016/j.petrol.2018.02.042

Wang, Z., Xu, K., and Zhang, H. (2022). Fracture Effectiveness Evaluation of Ultra-deep Tight Sandstone Reservoirs: A Case Study of the Keshen Gas Field, Tarim Basin, West China. *Front. Earth Sci.* 10, 883479. doi:10.3389/feart.2022.883479

Xiao, Z., Ding, W., Hao, S., Taleghani, A. D., Wang, X., Zhou, X., et al. (2019b). Quantitative Analysis of Tight Sandstone Reservoir Heterogeneity Based on Rescaled Range Analysis and Empirical Mode Decomposition: A Case Study of the Chang 7 Reservoir in the Dingbian Oilfield. *J. Petroleum Sci. Eng.* 182, 106326. doi:10.1016/j.petrol.2019.106326

Xiao, Z., Ding, W., Liu, J., Tian, M., Yin, S., Zhou, X., et al. (2019a). A Fracture Identification Method for Low-Permeability Sandstone Based on R/S Analysis and the Finite Difference Method: A Case Study from the Chang 6 Reservoir in Huaqing Oilfield, Ordos Basin. *J. Petroleum Sci. Eng.* 174, 1169–1178. doi:10.1016/j.petrol.2018.12.017

Xue, Y., Cheng, L., Mou, J., and Zhao, W. (2014). A New Fracture Prediction Method by Combining Genetic Algorithm with Neural Network in Low-Permeability Reservoirs. *J. Petroleum Sci. Eng.* 121 (2), 159–166. doi:10.1016/j.petrol.2014.06.033

Yang, H., Pan, H., Wu, A., Luo, M., Konaté, A. A., and Meng, Q. (2017). Application of Well Logs Integration and Wavelet Transform to Improve Fracture Zones Detection in Metamorphic Rocks. *J. Petroleum Sci. Eng.* 157, 716–723. doi:10.1016/j.petrol.2017.07.057

Yang, R., Ding, W., Liu, J., Zhao, Z., Li, S., and Xiao, Z. (2020). Fracture Identification of Ordovician Carbonate Reservoir Based on R/S Analysis in the North of the Shunbei No. 5 Fault Zone, Tarim Basin. *Interpretation* 8, T907–T916. doi:10.1190/int-2019-0284.1

Yang, Y., Tang, L., Diao, X., and Xie, D. (2018). Differential Deformation and its Control Mechanism of Fault Structures in Yakela Fault-Salient, Tarim Basin. *Oil Gas Geol.* 039 (001), 89–97. (in Chinese with English abstract). doi:10.11743/ogg20180109

Yin, S., Dong, L., Yang, X., and Wang, R. (2020). Experimental Investigation of the Petrophysical Properties, Minerals, Elements and Pore Structures in Tight Sandstones. *J. Nat. Gas Sci. Eng.* 76, 103189–103214. doi:10.1016/j.jngse.2020.103189

Yin, S., Lv, D., and Ding, W. (2018a). New Method for Assessing Microfracture Stress Sensitivity in Tight Sandstone Reservoirs Based on Acoustic Experiments. *Int. J. Geomechanics* 18 (4), 1–16. doi:10.1061/(asce)gm.1943-5622.0001100

Yin, S., and Wu, Z. (2020). Geomechanical Simulation of Low-Order Fracture of Tight Sandstone. *Mar. Petroleum Geol.* 117, 104359–104416. doi:10.1016/j.marpetgeo.2020.104359

Yin, S., Zhao, J., Wu, Z., and Ding, W. (2018b). Strain Energy Density Distribution of a Tight Gas Sandstone Reservoir in a Low-Amplitude Tectonic Zone and its Effect on Gas Well Productivity: a 3d Fem Study. *J. Petroleum Sci. Eng.* 170, 89–104. doi:10.1016/j.petrol.2018.06.057

Zhao, G., Ding, W., Sun, Y., Wang, X., Tian, L., Liu, J., et al. (2020). Fracture Development Characteristics and Controlling Factors for Reservoirs in the Lower Silurian Longmaxi Formation Marine Shale of the Sangzhi Block, Hunan Province, China. *J. Petroleum Sci. Eng.* 184, 106470. doi:10.1016/j.petrol.2019.106470

Zhao, K. K., Jiang, P. F., Feng, Y. J., Sun, X. D., Cheng, L. X., and Zheng, J. W. (2021). Investigation of the Characteristics of Hydraulic Fracture Initiation by Using Maximum Tangential Stress Criterion. *J. Min. Strata Control Eng.* 3 (2), 023520. doi:10.13532/j.jmsce.cn10-1638/td.20201217.001

Zheng, H., Wu, M., and Wu, X. (2007). Oil-gas Exploration Prospect of Dolomite Reservoir in the Lower Paleozoic of Tarim Basin. *Acta Pet. Sin.* 28 (2), 1–8. doi:10.3321/j.issn:0253-2697.2007.02.001

Zheng, H., Zhang, J., and Qi, Y. (2020). Geology and Geomechanics of Hydraulic Fracturing in the Marcellus Shale Gas Play and Their Potential Applications to the Fuling Shale Gas Development. *Energy Geosci.* 1 (1–2), 36–46. doi:10.1016/j.engeos.2020.05.002

Zheng, R. C., Zhong, G, H. U., and Feng, Q. P., (2007). Genesis of Dolomite Reservoir of the Changxing Formation of Upper Permian,northeast Sichuan Basin. *J. Mineralogy Petrology*, 27(4), 78–84. doi:10.1016/S1872-5813(08)60001-8

Zhongying, Z., Yulin, W., Guangdi, L., and Xiang, S. (2011). An Rescaled Range Analysis on the Characteristics of Coal Seam Development in the Eastern Depression of the Liaohe Basin. *Min. Sci. Technol. (China)* 21 (02), 223–227. doi:10.1016/j.mstc.2011.02.011

Zhou, X., Wang, R., and Du, Z. (2022). Characteristics and Main Controlling Factors of Fractures within Highly-Evolved Marine Shale Reservoir in Strong Deformation Zone. *Front. Earth Sci.* 10, 832104. doi:10.3389/feart.2022.832104

Zhou, Y., Yang, F., Ji, Y., Zhou, X., and Zhang, C. (2020). Characteristics and Controlling Factors of Dolomite Karst Reservoirs of the Sinian Dengying Formation, Central Sichuan Basin, Southwestern china. *Precambrian Res.* 343, 105708. doi:10.1016/j.precamres.2020.105708

Zhu, G., Milkov, A. V., Li, J., Xue, N., Chen, Y., Hu, J., et al. (2021). Deepest Oil in Asia: Characteristics of Petroleum System in the Tarim Basin, china. *J. Petroleum Sci. Eng.* 199, 108246. doi:10.1016/j.petrol.2020.108246

Conflict of Interest: Author XD was employed by the Sinopec Northwest Oilfield Company.

The remaining authors declare that the research was conducted in the absence of any commercial or financial relationships that could be construed as a potential conflict of interest.